

Provided for non-commercial research and education use.
Not for reproduction, distribution or commercial use.



This article appeared in a journal published by Elsevier. The attached copy is furnished to the author for internal non-commercial research and education use, including for instruction at the authors institution and sharing with colleagues.

Other uses, including reproduction and distribution, or selling or licensing copies, or posting to personal, institutional or third party websites are prohibited.

In most cases authors are permitted to post their version of the article (e.g. in Word or Tex form) to their personal website or institutional repository. Authors requiring further information regarding Elsevier's archiving and manuscript policies are encouraged to visit:

<http://www.elsevier.com/copyright>



Contents lists available at ScienceDirect

Journal of Sound and Vibration

journal homepage: www.elsevier.com/locate/jsvi

Vibration analysis of long cylindrical shells using acoustical excitation

Anooshiravan Farshidianfar^{a,*}, Mohammad H. Farshidianfar^a, Malcolm J. Crocker^b, Wesley O. Smith^b^a Department of Mechanical Engineering, Ferdowsi University of Mashhad, Mashhad, Iran^b Department of Mechanical Engineering, Auburn University, Auburn, USA

ARTICLE INFO

Article history:

Received 22 September 2010

Received in revised form

3 February 2011

Accepted 3 February 2011

Handling Editor: H. Ouyang

Available online 24 February 2011

ABSTRACT

Acoustical excitation along with two other methods was used to excite a long circular cylindrical shell, with simply supported boundary conditions. By comparing different types of excitation, the acoustical method was discovered to have many advantages over other methods of excitation used by previous researchers. Five different analytical methods based on the Love and Flugge theories, were also studied. The objective of this study was to identify the accuracy of each theory, in predicting the natural frequencies and mode shapes of a long circular cylindrical shell. A study was made to compare the predictions of the five analytical methods with experimental measurements. Interesting theoretical and experimental observations were observed for the long shell. Finally, a simple method is proposed to reduce the errors found in some of the analytical methods.

© 2011 Elsevier Ltd. All rights reserved.

1. Introduction

Many engineering structures have the basic form of thin-walled circular cylindrical shells; for example, pipes and ducts, aircraft fuselages, fluid storage tanks, submarine pressure hulls, electric motor and generator casings and some musical instruments. In many cases of long, slender cylinders having relatively thick walls, only transverse bending, beam-like modes of propagation, in which distortion of the cross section is negligible, are of practical interest. This is particularly true for low-frequency vibration of pipes in industrial installations such as petro chemical plants.

However, if the ratio of cylinder radius to wall thickness is large, as in aircraft fuselages, wave propagation involving distortion of the cross section is of practical importance even at relatively low audio frequencies. The analysis of vibration characteristics of thin-walled circular cylindrical shells is more complex than that of beams and plates. This is mainly because the equations of motion of cylindrical shells together with boundary conditions are more complex.

Much of the technical literature in the past century has been focused on the analysis of thin-walled structures, and many studies were concerned with cylindrical shells that constitute the main parts of aircrafts, rockets and generally aerospace structures.

The literature concerning the vibration of shells is extremely extensive and readers can refer to Leissa [1] or more recently Amabili and Paidoussis [2] for comprehensive reviews of models and results presented in the literature. In the following, some studies, strictly related to the present study are described.

* Corresponding author.

E-mail address: farshid@um.ac.ir (A. Farshidianfar).

Nomenclatures	
$a_i (i=0, 2, 4)$	coefficients of Love characteristic equation
A'', I	area and inertia moment of beam cross section
A, B, C	modal (wave) amplitudes in axial, circumferential and radial directions, respectively
C	speed of sound wave in air
E	Young's modulus of elasticity
F	frequency of sound wave
H	shell thickness
k_a	non-dimensional axial wavenumber
k_m	axial wavenumber
$K_i (i=1, 2, 3, 4)$	real parts of characteristic equation roots
L	shell length
$L_i (i=1, \dots, 6)$	partial differential operators
M	longitudinal wave parameter
N	circumferential wave parameter
$p_i (i=2, 4, 6)$	and Δp_0 coefficients of Flugge characteristic equation
$q_i (i=0, 2, 4, 6)$	coefficients of characteristic equation
R	shell radius
u, v, w	axial, circumferential and radial components of displacement, respectively
x	longitudinal coordinate of shell
β	non-dimensional thickness parameter
θ	circumferential coordinate of shell
λ	wavelength of sound wave
ρ	mass density
ν	Poisson's ratio
ω	circular natural frequency
Ω	non-dimensional frequency parameter
<i>Subscripts</i>	
wp	wave propagation approach
y	Yu's simplification

Love [3] modified the Kirchhoff hypothesis for plates and established the assumptions used in the so-called classic theory of thin shells. These assumptions are now commonly known as Love's approximation of the first kind. Love then subsequently formulated a shell theory known as Love's first approximation theory and the assumptions he established soon became the foundations on which many thin shell theories were later developed, such as the Flugge theory [4].

Soedel [5] introduced a set of three closed form solutions for the natural frequencies of cylindrical shells and also obtained mode shape coefficients of a simply supported cylindrical shell by applying normal solutions to the Love theory [3]. Forsberg [6] applied energy methods to the Flugge theory and considered the effects of tangential inertia.

Over the past few years, the use of the wave propagation approach has also attracted considerable attention. Harari [7] first studied the wave propagation in shells with a wall joint. Fuller [8] considered the effects of wall discontinuities on the propagation of flexural waves. Zhang [9] treated mode shapes of the cylindrical shell as combinations of standing waves both in axial and circumferential directions, and more recently the wave propagation approach was used by Li [10] for the free vibration analysis of circular cylindrical shells based on the classical Flugge theory.

In addition to the direct solutions, many researchers have used certain simplifications and derived much simpler characteristic equations. There are two widely used simplifications discussed in the literature: (1) by Yu [11] and (2) by Forsberg [6] in which he neglected the tangential inertia terms of a cylindrical shell. Yu showed that for a cylindrical shell in which the circumferential wavelength is much less than the axial one, the characteristic equation is similar to that of a lateral vibrating Euler–Bernoulli beam. Applying his simplification to the Donell theory along with the neglect of tangential inertia, Yu was able to come up with some good results. Such a procedure was similarly carried out by Weingarten [12]. As mentioned above, a further investigation of the neglect of tangential inertia and its effects on theoretical results was carried out by Forsberg.

Although all these theoretical methods are compared to the exact analysis in order to study their accuracy, one should bear in mind that all these methods including the exact analysis assume perfect boundary conditions, which are not found in the real world. Therefore, apart from the theoretical aspects of shell vibrations, there has also been many experimental studies made, see, e.g., Refs. [13–15], for comparison with theoretical predictions. The majority of these experiments have been made on shells with small length/radius ratios. The literature shows that in all of the experimental efforts developed for investigating vibration, techniques such as; the impact method (use of a hammer) and the impedance head method (use of a shaker) were utilized in the measurements. All these methods of excitation are contact techniques and have some effects in the form of mass loading on the frequency response function of the system.

The main aim of the present paper is to investigate the advantages of applying acoustical excitation over the more traditional contact excitations (shaker, hammer, etc.) used in the past. Unlike beams which are one-dimensional structures, a shell can vibrate in three directions. It was found in previous studies [14], that contact excitations employed previously were not able to excite all the modes in all these three directions simultaneously. Hence by applying acoustical excitation to a long cylindrical shell, better results were obtained. Not only was acoustical excitation able to excite all the modes, but it was also found out to have many more advantages over contact excitation methods. Moreover, many of experimental studies conducted in the past were applied to short or medium length shells. Therefore a long shell with a length/radius ratio of 22.67 was selected for investigation in the present study. Theoretical results were obtained according to five various theories mentioned above. By comparison with experimental results, the

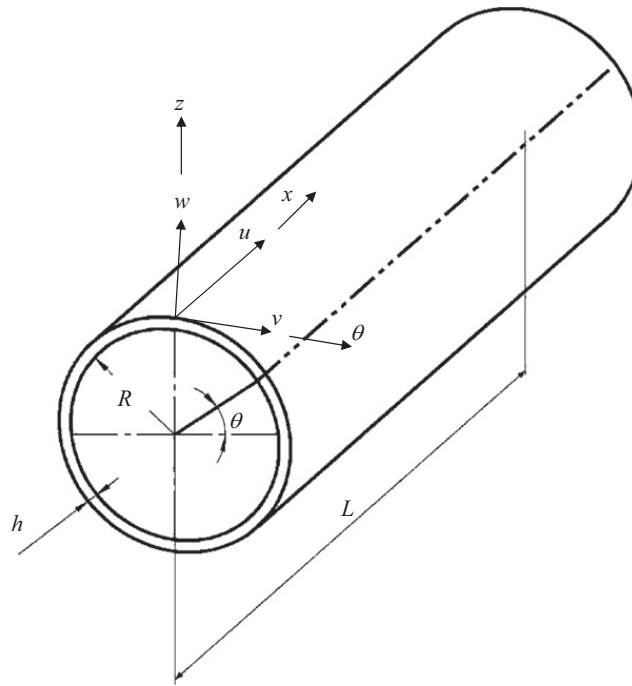


Fig. 1. Circular cylindrical shell: coordinate system and dimensions.

validation of each theory and the experimental approaches were examined, for the case of long cylindrical shells. It was found out that some theories did not respond accurately enough to a shell with such dimensions. Therefore a simple method is proposed to reduce errors. Some interesting experimental observations were also noticed which will be discussed later on.

2. Formulation of problem

Let us consider a shell having constant thickness h , mean radius R , axial length L , Poisson's ratio ν , density ρ and Young's modulus of elasticity E . Shell coordinates are taken longitudinally in the x -direction and circumferentially in the θ -direction, respectively, shown in Fig. 1.

The equations of motion for a cylindrical shell can be written in matrix form as follows:

$$\begin{bmatrix} L_{11} & L_{12} & L_{13} \\ L_{21} & L_{22} & L_{23} \\ L_{31} & L_{32} & L_{33} \end{bmatrix} \begin{Bmatrix} u \\ v \\ w \end{Bmatrix} = 0 \quad (1)$$

where u , v and w are orthogonal directions, respectively, in the axial, circumferential and radial directions, shown in Fig. 1, and $L_{ij}(i,j=1, 2, 3)$ are differential operators with respect to x and θ . The matrix differential operators differ for each theory. Differential operators based on the Love and Flugge theory are presented in Appendix A.

Since the shell has a uniform wall thickness, the allowable spatial form of distortion of a cross section must be periodic in the length of the circumference. The axial, tangential and radial displacements of the wall vary according to

$$\begin{cases} u = A \cos(k_m x) \cos(n\theta) \cos(\omega t) \\ v = B \sin(k_m x) \sin(n\theta) \cos(\omega t) \\ w = C \sin(k_m x) \cos(n\theta) \cos(\omega t) \end{cases} \quad (2)$$

in which k_m and n are the axial wavenumber and the circumferential wave parameter, respectively, A , B and C are, respectively, the modal (wave) amplitudes in the x , θ and z directions, and ω is the circular driving frequency.

3. Flugge theory

Substituting Eq. (2) into the Flugge theory discussed earlier, a set of homogenous equations having the following matrix form is yield:

$$\begin{bmatrix} C_{11} & C_{12} & C_{13} \\ C_{21} & C_{22} & C_{23} \\ C_{31} & C_{32} & C_{33} \end{bmatrix}_F \begin{Bmatrix} A \\ B \\ C \end{Bmatrix} = \begin{Bmatrix} 0 \\ 0 \\ 0 \end{Bmatrix} \quad (3)$$

in which $[C_{ij}]_F (i,j=1, 2, 3)$ are functions of n, k_m and ω . For nontrivial solution the determinant of the coefficient matrix in Eq. (3) must be zero:

$$\det([C_{ij}]_F) = 0, \quad i,j = 1, 2, 3 \tag{4}$$

The expansion of Eq. (4) will give the characteristic equation and for a particular value of n , the characteristic equation yields either of the following eigenvalue problems:

- For a given value of k_m there exists one or more proper values for ω so that the determinant vanishes.
- For a given value of ω there exists one or more proper values for k_m so that the determinant vanishes.

So, if an initial driving frequency ω is given, a bi-fourth polynomial equation with respect to k_m could be calculated as follows:

$$k_m^8 + q_6 k_m^6 + q_4 k_m^4 + q_2 k_m^2 + q_0 = 0 \tag{5}$$

where $q_i (i=0, 2, 4, 6)$ are functions of ω and n . For the usual range of parameters and $n \geq 1$, the roots of Eq. (5) have the form:

$$k_m = \pm K_1, \pm iK_2, \pm (K_3 \pm iK_4) \tag{6}$$

where $K_i (i=1, \dots, 4)$ are real positive numbers dependent on the driving frequency ω . The linear summation of all eight roots, would gain mode shape in the u, v and w coordinates. For all these eight unknowns to be calculated one has to employ eight boundary conditions, four at each end. Depending upon the boundary conditions employed, a set of eight homogenous equations is expressed as follows:

$$[\mathbf{H}]_{8 \times 8} \{\mathbf{b}\}_{3 \times 1} = \{0\} \tag{7}$$

in which ω and $b_i (i=1, \dots, 8)$ are the nine unknowns. For a nontrivial solution of Eq. (7) one requires:

$$\det([\mathbf{H}]) = 0 \tag{8}$$

The driving frequencies are obtained by solving Eq. (8). The other 8 unknowns are solved by substituting these frequencies into Eq. (7).

3.1. Direct solution analysis

The exact method of above equation is a very long and a complicated procedure, and because of its lengthy calculations more errors are produced. Thus a different approach is proposed by assuming the axial wavenumber k_m and the circumferential wave parameter n of the corresponding natural frequency to be known. Such method yields a new characteristic equation for the Flugge theory, having the following form [1]:

$$\Omega^6 - (p_4)\Omega^4 + (p_2)\Omega^2 - (p_0) = 0 \tag{9}$$

where

$$\Omega^2 = \frac{\rho(1-\nu^2)R^2\omega^2}{E}, \quad \beta = \frac{h^2}{12R^2} \tag{10}$$

represent the non-dimensional frequency parameter and the non-dimensional thickness parameter, respectively. In the above equations $p_i (i=0, 2, 4)$, are functions of k_m and n , which will be treated as known variables. Coefficients of the characteristic equation, according to the direct solution of the Flugge theory are given in Appendix A. Therefore by predicting a determined mode shape for the shell, which will be discussed later on, the corresponding driving frequency will be found. For a combination of k_m and n , bi-cubic Eq. (9) would have three positive roots. A shell of a given length may vibrate in any of these three frequencies with all of them having the same longitudinal and circumferential wavenumbers. Therefore in a cylindrical shell every mode shape has three distinct natural frequencies; however, the modes associated with each of these frequencies can be classified as primarily radial (or flexural), longitudinal (or axial) or circumferential (or torsional). Usually the lowest frequency is associated with a motion that is primarily radial. Nevertheless, depending upon shell dimensions, some low frequency modes are recognized as primarily longitudinal or circumferential rather than radial. As an example, for long shells which behave more like a beam rather than a ring, some low frequency modes are associated with axial dominant motions. Such modes produce bending motions in a long shell.

4. Love theory

By substituting Eq. (2) into the Love's equations of motion and undergoing a process similar to that of the above, a set of homogenous equations is obtained, as follows:

$$\begin{bmatrix} C_{11} & C_{12} & C_{13} \\ C_{21} & C_{22} & C_{23} \\ C_{31} & C_{32} & C_{33} \end{bmatrix}_L \begin{Bmatrix} A \\ B \\ C \end{Bmatrix} = \begin{Bmatrix} 0 \\ 0 \\ 0 \end{Bmatrix} \quad (11)$$

For nontrivial solutions, one sets the determinant of the coefficient matrix in Eq. (11) equal to zero and the following characteristic equation is obtained [5]:

$$\Omega^6 + a_4\Omega^4 + a_2\Omega^2 + a_0 = 0 \quad (12)$$

The solutions of the above equation are similar to [5]:

$$\Omega_{1mn}^2 = -\frac{2}{3}\sqrt{a_4^2 - 3a_2} \cos \frac{\alpha}{3} - \frac{a_4}{3} \quad (13)$$

$$\Omega_{2mn}^2 = -\frac{2}{3}\sqrt{a_4^2 - 3a_2} \cos \frac{\alpha + 2\pi}{3} - \frac{a_4}{3} \quad (14)$$

$$\Omega_{3mn}^2 = -\frac{2}{3}\sqrt{a_4^2 - 3a_2} \cos \frac{\alpha + 4\pi}{3} - \frac{a_4}{3} \quad (15)$$

in which

$$\alpha = \cos^{-1} \frac{27a_0 + 2a_4^3 - 9a_4a_2}{2\sqrt{(a_4^2 - 3a_2)^3}} \quad (16)$$

The coefficients of the Love characteristic equation $a_i (i=0, 2, 4, 6)$, are given in Appendix A. Similar to that of the Flugge theory, Love's characteristic equation (Eq. (12)) also has three positive roots. Therefore all statements expressed for the Flugge characteristic equation (Eq. (9)) are true for the Love's equation (Eq. (12)) likewise.

5. Mode shape identification

Mode shapes (or eigenfunctions) are identified by returning to the homogenous set of equations (Eqs. (3) and (11)), which yield the characteristic equation. By choosing any of the two homogenous equations and discarding the third, the modal amplitude ratios of Eq. (2) are obtained. The two homogenous functions are usually depicted in a way so that the modal amplitude ratios; A/C and B/C could be obtained.

For example by considering the first two equations of Eq. (11), and solving the amplitudes A and B in terms of C one would have:

$$\begin{bmatrix} \rho h \omega_{imn}^2 - t_{11} & t_{12} \\ t_{21} & \rho h \omega_{imn}^2 - t_{22} \end{bmatrix} \begin{Bmatrix} \frac{A_i}{C_i} \\ \frac{B_i}{C_i} \end{Bmatrix} = - \begin{Bmatrix} t_{13} \\ t_{23} \end{Bmatrix} \quad (17)$$

where $\Omega_{imn} (i=1, 2, 3)$ are provided by Eqs. (13), (14) and (15). By solving Eq. (17) the final expressions for A_i/C_i and B_i/C_i terms can be found as in [5]:

$$\frac{A_i}{C_i} = -\frac{t_{13}(\rho h \Omega_{imn}^2 - t_{22}) - t_{12}t_{23}}{(\rho h \Omega_{imn}^2 - t_{11})(\rho h \Omega_{imn}^2 - t_{22}) - t_{12}^2} \quad (18)$$

and

$$\frac{B_i}{C_i} = -\frac{t_{23}(\rho h \Omega_{imn}^2 - t_{11}) - t_{21}t_{13}}{(\rho h \Omega_{imn}^2 - t_{11})(\rho h \Omega_{imn}^2 - t_{22}) - t_{12}^2} \quad (19)$$

As indicated above, the lowest of the three natural frequencies for each k_m and n combination usually yields A_i/C_i and B_i/C_i ratios, less than unity, indicating primarily radial motion.

6. Wave propagation approach

Shell displacements can be expressed in the form of wave propagation as

$$\begin{cases} u = A_{wp}(e^{-ik_m x}) \cos(n\theta)(e^{i\omega t}) \\ v = B_{wp}(e^{-ik_m x}) \sin(n\theta)(e^{i\omega t}) \\ w = C_{wp}(e^{-ik_m x}) \cos(n\theta)(e^{i\omega t}) \end{cases} \quad (20)$$

By substituting Eq. (20) into the Flugge equations of motion (Eq. (1)) the following characteristic equation is provided [10]:

$$\Omega^6 + (p_4)_{wp}\Omega^4 + (p_2)_{wp}\Omega^2 + (p_0)_{wp} = 0 \quad (21)$$

Eq. (21) has the same arrangement as the direct solution of the Flugge theory (Eq. (9)), however with different characteristic coefficients $(p_i)_{wp}(i=0, 2, 4)$.

7. Axial and circumferential wave parameter identification

In order to calculate natural frequencies, it is only necessary to determine the wavenumber, k_m in the axial direction, and the circumferential wave parameter, n . The parameter n , should always be taken as an integer number and independent from the boundary conditions imposed. However, as Eqs. (5) and (7) imply, k_m strongly depends upon the boundary conditions employed. The values of k_m are found by the set of eight homogenous equations shown in Eq. (7), and to obtain these equations one has to solve the equations of motion with appropriate boundary conditions. For flexural vibrations, one may use the beam functions to determine the axial wavenumbers of cylindrical shells. The flexural mode shapes of cylindrical shells in the axial direction are assumed to be of the same form as a transversely vibrating beam, with the same boundary conditions. The utilization of beam functions has been of broad use over the past [1,5], and more recently in the wave propagation approach [9,10]. From Eqs. (9), (12) and (21), one can notice that the axial wavenumber k_m , and the circumferential wave parameter n , are the only unknowns in all these characteristic equations. Therefore, the results of a vibrating beam along with integer numbers of n are directly substituted into these characteristic equations (Eqs. (9), (12) and (21)), and the natural frequencies are obtained.

Modal wavenumbers in the axial direction of the circular cylindrical shell for different boundary conditions are presented in Table 1. These modal wavenumbers are according to the beam functions with the same boundary conditions.

For cylindrical shells with simply supported boundary conditions, typical flexural, longitudinal and circumferential nodal patterns according to different m and n combinations are shown in Fig. 2.

8. Simplified approximate methods

As noticed above, the characteristic equations acquired by the direct solution, involve the combination of many complicated terms. Although such complexity may not seem bothering for the case of simple edge conditions, but, for more complicated boundary conditions such as; point supports, solving these equations will endure the need of sophisticating calculations. Moreover, such complex sixth-order polynomial equations are of no interest to practical engineers. Therefore many simplifications are proposed to either; (1) the equations of motion or (2) the final characteristic equation itself. By employing such simplifications, simple or closed-form solutions of the natural frequencies are obtained.

8.1. Neglect of tangential inertia

The lowest natural frequencies of a cylindrical shell are usually dominant in the radial direction, hence for such modes, one may assume the tangential displacements to be relatively small. Considering such an assumption an important simplification is frequently applied, by neglecting the tangential inertia terms in the equations of motion. In this procedure the shell mass is treated as if it has three components; with the inplane components neglected (equaled to zero). The first and the most obvious consequence of neglecting tangential inertia terms in the equations of motion, is the reduction of the

Table 1
Shell axial wavenumbers according to beam functions.

Wavenumber and boundary conditions		
Shell boundaries	Wavenumber	Boundary conditions
Simply supported–simply supported (SS_SS)	$k_m = \frac{m\pi}{l}$	$v=w=N_x=M_x=0, x=0,l$
Clamped–clamped (C_C)	$k_m = \frac{(2m+1)\pi}{2l}$	$u=v=w=\frac{\partial w}{\partial x}=0, x=0,l$
Clamped–simply supported (C_SS)	$k_m = \frac{(4m+1)\pi}{4l}$	$u=v=w=\frac{\partial w}{\partial x}=0, x=0 v=w=N_x=M_x=0,x=l$

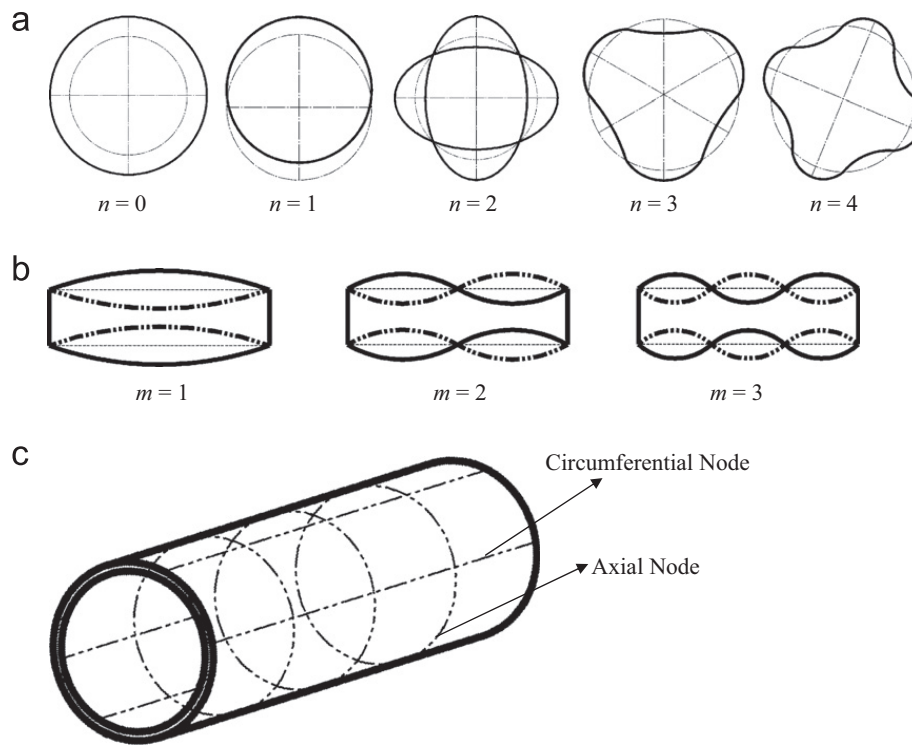


Fig. 2. Mode shapes of a cylindrical shell: (a) circumferential mode shapes; (b) longitudinal and radial mode shapes; and (c) nodal arrangement of a cylindrical shell for $n=2, m=4$.

frequency characteristic equation, from a cubic to a first-order expression. Thus two of the three frequencies are no longer present and only one frequency would be left. The retained frequency is the one associated with a primarily radial motion.

By applying this procedure to the Flugge equations of motion, the following closed-form solution is obtained [1]:

$$\Omega^2 = \frac{p_0}{p_2} \quad (22)$$

in which p_0 is the same as the one used in Eq. (9).

8.2. Yu's simplification

Another type of simplification was introduced by Yu [11], by considering a non-dimensional axial wavenumber written as follows:

$$k_a = Rk_m \quad (23)$$

In this simplification, when the circumferential wavelength is small compared to the axial wavelength:

$$\frac{k_a^2}{n^2} \ll 1 \quad (24)$$

one could neglect k_a^2 relative to n^2 terms in the characteristic equation. Here, k_a^2/n^2 is called as wavelength ratio. So, by applying such a simplification to the Flugge characteristic equation (Eq. (9)), the following simplified equation is concluded:

$$\Omega^6 + (p_4)_y \Omega^4 + (p_2)_y \Omega^2 + (p_0)_y = 0 \quad (25)$$

9. Experimental setup

Tests were conducted on a circular cylindrical shell made of aluminum with material properties; $E=68.2$ GPa, $\rho = 2700 \text{ kg/m}^3$ and $\nu=0.33$. Dimensions of the shell and the experimental setup are shown in Figs. 3 and 4. Two steel disks with external radii of 76.2 mm were inserted into both ends of the shell, each fastened tightly by two fastening chains to produce simply supported boundary conditions. The end disks were intentionally chosen heavy, in order to prevent rigid body motion of the shell. Fastening chains were also used to forbid outward displacements of the shell ends.

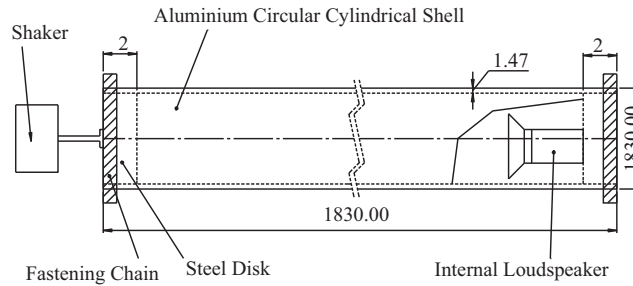


Fig. 3. Schematic view and dimensions of the system analyzed experimentally (all dimensions are given in millimeters).

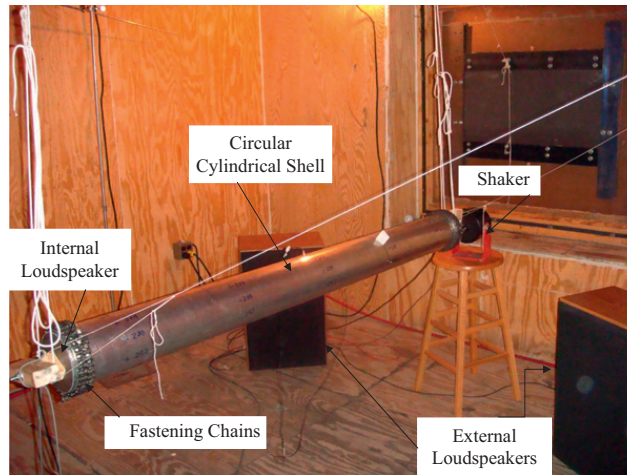


Fig. 4. Experimental setup and excitation techniques.



Fig. 5. Internal loudspeaker setup.

The shell body had a longitudinal welded seam which was machined by a lathe so that a leveled and perfect surface would be obtained (Fig. 4). The cylinder was then subjected to two general methods of excitation:

- (1) Contact excitation divided into:
 - (a) The impedance head method, which is using a shaker (B and K type 4809, 60 N peak force, 100 g maximum acceleration, frequency band of 10 Hz–20 kHz).
 - (b) The impact method, which is using a modal hammer (Endevco type 2302, 4448 N maximum force, maximum frequency 8 kHz).
- (2) Noncontact (acoustical) excitation divided into:
 - (a) External loudspeakers (Pioneer CS-G405Q, cross over frequencies of 2.4 kHz–10 000 kHz).
 - (b) Internal loudspeaker (Fig. 5).

The whole shell setup was put into a reverberant room in order to make the sound pressure equal at all surface points, inside and outside the shell, so that the acoustical excitation could easily excite axisymmetric ($n=0$) modes of the shell. These modes are hard to excite by other types of excitation. The idea behind using four different methods of excitation was to find the best way to excite all modes simultaneously. A full comprehensive and a comparative study of the different methods of excitation applied is discussed in the next section.

60 measurement points were uniformly distributed over the shell's length and circumference in order to identify various mode shapes. The shell response was then measured using two accelerometers; (Endevco accelerometer type 2226C, mass of 2.8 g and B and K accelerometer type 4375, mass of 2.4 g), each connected to a B and K 2647B charge amplifier. All transducers and exciters were connected to a 3560 Pulse Multi Analyzer System. Measurements were analyzed using Pulse Software 10.1.

In order to find natural frequencies, measurements were carried out over several points and a simple FFT (with 100 averages over a time domain) was evaluated for every point. A Matlab program was used to plot circumferential and longitudinal mode shapes. Because of the high modal density and certain excitation problems, it was difficult for some methods of excitation to excite certain modes at some frequency ranges.

9.1. Methods of excitation

A shell with such dimensions; $L/R=22.67, R/h=51.72$, is more complex than other cases, because this system exhibits; (1) axisymmetric ($n=0$), (2) beam-like ($n=1$) and (3) asymmetric ($n > 1$) modes, all in low ranges of frequency (0–1000 Hz). Therefore the type of excitation employed and its capability in exciting all such modes is of great importance. Each method of excitation had certain advantages and disadvantages; however, after a comparison of all methods a good conclusion was gained. A point near the left end was chosen and all FFTs are reported for this point. Modes obtained by each method were then compared with theoretical results to find the best method, able to excite all modes. A wide frequency range of 0–3200 Hz was chosen in order to see the response of each method both at low and high frequencies. It should be mentioned that all natural frequencies below the 1000 Hz frequency range have been calculated by theory. Therefore, if additional information is needed, one can refer to Table 2 in which all experimental and theoretical results are reported for the frequency range 0–1000 Hz.

Both contact methods (the shaker and the modal hammer) were applied to the ends of the shell (forces were applied to end steel disks), therefore an axial force was applied to the shell. These points were chosen because of their capability of pumping energy uniformly, throughout the shell's whole circumference and length. Hence by using these specific exciting points, excitation of axisymmetric modes along with beam-like and asymmetric modes is made easy.

Both of the two contact excitations were applied to the left end of the shell. The two excitations mentioned are the most practical used by former researchers for vibration analysis of thin-walled structures. However, when confronted by a similar shell having all three mode types (axisymmetric, beam-like and asymmetric), none of the above methods were

Table 2

Comparison between theoretical and experimental results of natural frequencies and mode shapes (0–1 kHz frequency range); $L/R=22.67, R/h=51.72$.

Longitudinal wave parameter <i>m</i>	Circumferential wave parameter <i>n</i>	Natural frequency (Hz)					
		Experiment	Flugge	Love	WP ^a (Flugge)	Simplified NTI ^b (Flugge)	Simplified Yu (Flugge)
1	1	138.40	138.88	138.93	198.86	197.85	142.63
1	2	190.30	172.83	172.94	194.88	193.40	172.16
2	2	310.50	244.8	244.78	283.27	274.16	245.25
3	2	496.60	423.76	424.15	517.61	476.60	438.75
1	3	502.20	471.38	471.46	498.99	497.03	470.42
2	3	477.00	481.24	481.44	516.22	507.67	477.58
3	3	558.90	514.06	514.47	565.69	542.72	507.41
2	1	464.70	517.95	518.02	778.31	749.05	572.99
4	3	638.30	586.02	586.64	673.61	619.29	580.19
4	2	679.80	687.78	688.23	922.83	775.88	741.75
5	3	782.00	705.25	706.05	871.43	746.05	709.69
6	3	833.80	869.68	870.62	1215.20	920.90	898.84
1	0	842.50	892.07	892.08	892.17	10497.00	-
1	4	884.40	902.20	902.29	932.32	930.14	901.15
2	4	887.00	906.59	906.75	944.07	934.82	902.39
3	4	981.60	917.05	917.34	969.10	945.87	907.77
4	4	945.80	937.82	938.28	1015.90	967.64	922.09
5	4	964.70	973.81	974.47	1097.90	1005.20	951.58

^a Wave propagation.

^b Neglect of tangential inertia.

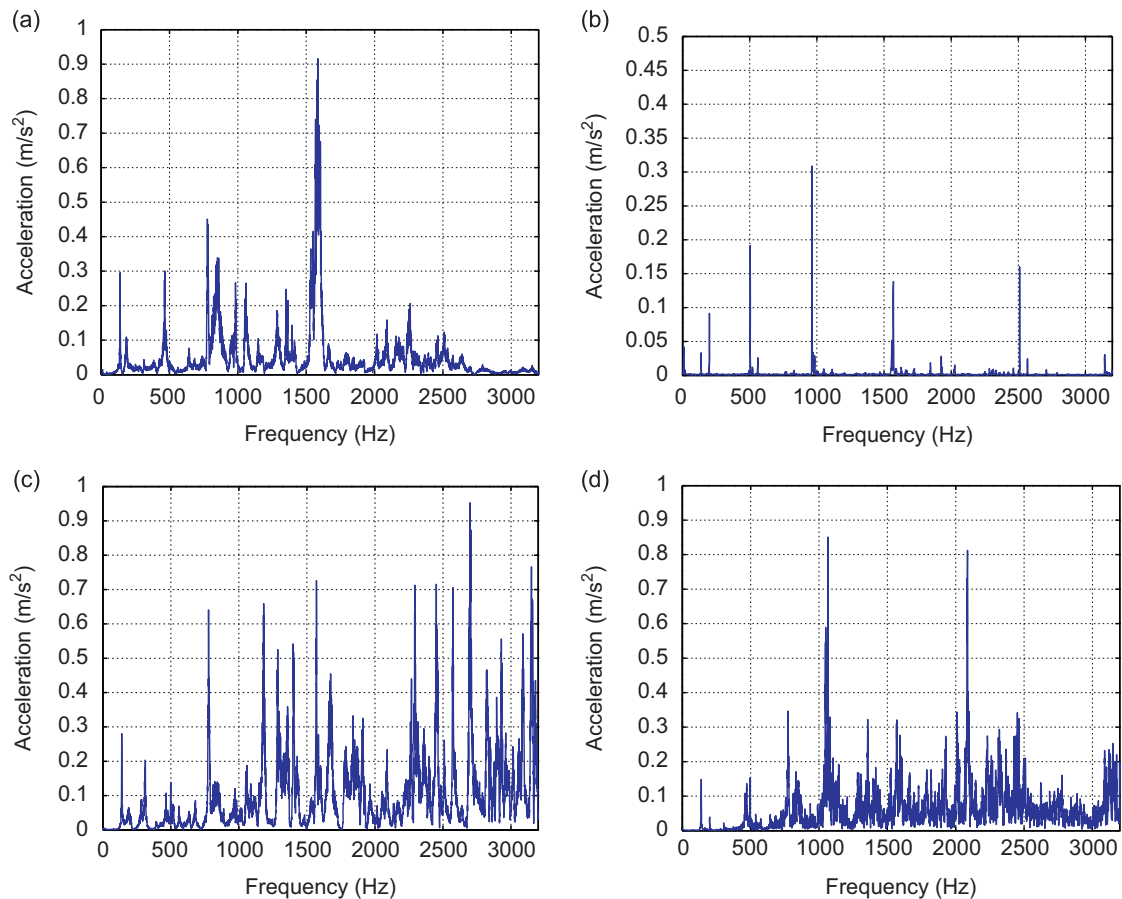


Fig. 6. FFT comparisons of each excitation method (0–32 000 Hz frequency range): (a) shaker; (b) modal hammer; (c) internal loudspeaker; and (d) external loudspeaker.

sufficient enough individually to capture and excite all modes in a certain frequency band. More recently Pellicano [14] encountered such a problem in which he used three different methods of excitation to excite all three mode groups.

The effect of acoustical excitation was investigated on shell vibrations. In the first case, two external loud speakers were utilized, each put at one end of the shell aligned with the shell's longitudinal axis in contribution to a symmetric setup. In the second case however, an internal speaker was connected to one of the steel ends with the whole setup inserted into the right end of the shell to produce simply supported condition. Internal speaker setup is shown in Fig. 5.

All experiments were performed in a reverberant room, thus sound pressure would be equal at all points inside and outside the shell. Such conditions produced uniformly distributed forces along longitudinal and circumferential directions of the shell resulting in easy excitation of axisymmetric modes along with all other modes. However, if one is not able to acquire the need for a reverberant room, it is not of great matter, because the internal speaker setup would have the same effect of an external speaker inside a reverberant room. This is due to the fact that, the inside of a cylindrical shell is a reverberant field by itself. Therefore, if sound waves are produced inside the shell (as in the case of an internal speaker), equal sound pressures are produced on the shell's surface. Hence, an internal speaker is recommended for a situation in which no reverberant room is available.

FFTs obtained by each method are presented in Fig. 6, and if noticed in the figure, the contact excitations produced different results compared with the acoustical excitations; missing several frequencies especially at high frequency bands.

It was observed in the frequency range 0–1000 Hz, that the shaker (Fig. 6a) was not able to excite some modes strongly enough, such as; $(m,n)=\{(2,2),(1,3),(3,2),(3,3)\}$, some of these modes were completely missed and others had really small peaks which may not be recognized as a natural frequency. Furthermore, because of the high modal density in the frequency band of 830–890 Hz, four very closely spaced modes appeared in this region; however, the shaker excitation was not able to show all these modes separately and only one of them was picked by the shaker and the other three including; $(m,n)=\{(6,3),(1,4),(2,4)\}$ did not appear in this frequency response.

The same conclusions can be stated for the modal hammer excitation (Fig. 6b), with even more frequencies being missed relative to the shaker excitation both at low and high frequencies. The low frequency modes which were not well excited by the modal hammer are $(m,n)=\{(2,2),(2,1),(2,3),(3,3),(4,3),(4,2),(5,3),(6,3),(1,0),(1,4),(2,4),(4,4)\}$.

According to the modal density diagrams of a circular cylindrical shell [16] one should yield more modes at higher frequency bands, however, vice versa of such a statement is observed in frequency responses produced by the contact excitation methods.

For the acoustical excitations, however, it is observed in Fig. 6c and d, that both internal and external loudspeakers were able to excite all low frequency modes with no difficulty and with good precision. Moreover, in the acoustical frequency response as the frequency increases the peaks become more clear and more easy to identify. This phenomenon is perfectly understandable by theory. According to the following formula for sound waves propagating in air:

$$\lambda = \frac{c}{f} \tag{26}$$

in which c , f and λ describe the speed of sound in air, the sound wave frequency and the sound wave length, respectively, it is apparent that as the sound wave frequency increases as the sound wavelength becomes shorter. Therefore, it would be easier for the sound waves to couple with the structural waves at high frequencies, in which shorter sound wavelengths are produced. So, it would be easier for the acoustical excitation to excite the high frequency modes rather than the low frequency ones. This statement may lead one to assume that at low frequencies with long sound wavelengths introduced by an acoustical excitation, the method might not be a good solution. However, it is seen in Fig. 6c and d that both acoustical excitations were able to excite all low frequency modes similar to the high frequency modes.

Besides, when the contact method is applied, there would always be some load (mass) effects, affecting the specimen as the contact is made. According to elementary vibration equations, natural frequencies are proportional to the inverse square root of the mass, therefore such mass effects from the contact exciter usually decrease natural frequencies measured experimentally. This prediction was observed in the experiment, by comparing natural frequencies yield by the contact and the acoustical excitations. However by using an acoustical (noncontact) excitation, such a problem does not occur and the frequencies are measured more precisely.

Moreover, many experiments have been carried out regarding flow induced vibration of circular cylindrical shells. In the majority of these experiments the shell is either filled or surrounded by water from inside or outside. In these experiments the shaker or the hammer should be kept dry. This is usually very time consuming, or even at some circumstances an unaccomplished task to do. Whereas by using an acoustical excitation this problem is completely solved and the measurements of empty and fluid-filled shells could be done simultaneously without any change in the experimental setup.

10. Results and discussions

The main objective of this analysis is to study the free vibration of long thin-walled cylindrical shells, based on experimental investigations. Two different methods of excitation, namely contact and noncontact methods were used. In order to demonstrate the validity of these methods, five different analytical approximate methods were selected for comparison. As mentioned in the former sections these methods are: (1) the Flugge theory, (2) the Love theory, (3) the wave propagation approach based on the Flugge theory, (4) the simplified Flugge theory based on the neglect of tangential inertia and finally (5) the simplified Flugge theory based on Yu's assumption. It is to note that all experimental measurements have been provided by using the internal acoustical excitation.

Fig. 7 shows the experimentally predicted spectrum of vibration for the thin-walled cylindrical shell which was excited by an internal loudspeaker. In Table 2, the experimental and all of the five approximate analytical results are presented. A relative error is defined as follows:

$$\text{Error}_\omega = \frac{\omega_{\text{exp}} - \omega_{\text{analytical}}}{\omega_{\text{exp}}} \times 100\% \tag{27}$$

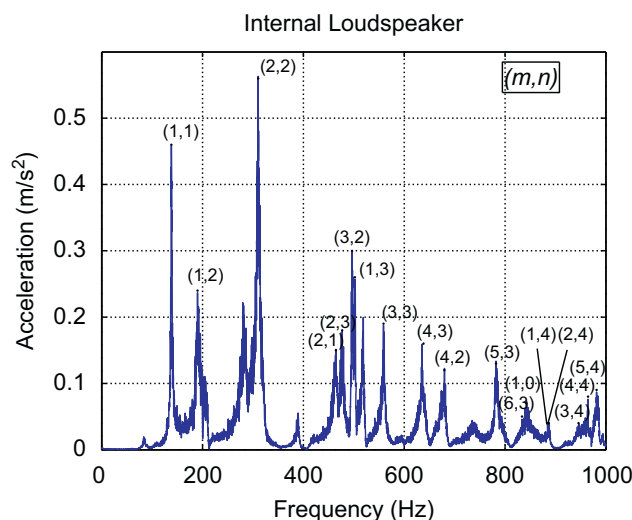


Fig. 7. Mode shape identification of natural frequencies: internal loudspeaker FFT (0–1000 Hz frequency range).

Table 3
Theoretical errors with respect to experimental results.

Longitudinal wave parameter <i>m</i>	Circumferential wave parameter <i>n</i>	Frequency (Hz) Experiment	Error (%)				
			Flugge	Love	WP ^a (Flugge)	Simplified NTI ^b (Flugge)	Simplified Yu (Flugge)
1	0	842.50	5.9	5.9	5.9	100	100
1	1	138.40	0.4	0.4	43.7	43.0	3.1
2	1	464.70	11.5	11.5	67.5	61.2	23.3
1	2	190.30	9.2	9.1	2.4	1.6	9.5
2	2	310.50	21.2	21.2	8.8	11.7	21.0
3	2	496.60	14.7	14.6	4.2	4.0	11.7
4	2	679.80	1.2	1.2	35.8	14.1	9.1
1	3	502.20	6.1	6.1	0.6	1.0	6.3
2	3	477.00	0.9	0.9	8.2	6.4	0.1
3	3	558.90	8.0	8.0	1.2	2.9	9.2
4	3	638.30	8.2	8.1	5.5	3.0	9.1
5	3	782.00	9.8	9.7	11.4	4.6	9.3
6	3	833.80	4.3	4.4	45.7	10.5	7.8
1	4	884.40	2.0	2.0	5.4	5.2	1.9
2	4	887.00	2.2	2.2	6.4	5.4	1.7
3	4	981.60	6.6	6.6	1.3	3.6	7.5
4	4	945.80	0.8	0.8	7.4	2.3	2.5
5	4	964.70	0.9	1.0	13.8	4.2	1.4

^a Wave propagation.
^b Neglect of tangential inertia.

in which subscripts ‘exp’ and ‘analytical’ represent the experimental and the approximate analytical methods, respectively. Error comparisons are given in Table 3.

The mode shape identification is of crucial importance in the case of shells, indeed, the high modal density makes it difficult to compare experimental and theoretical modes using natural frequencies only, therefore, the visualization is mandatory. In Fig. 8 mode shapes are reported for both experimental and analytical methods. The first mode, which is the fundamental mode, is a beam-like mode.

Comparisons reported in Table 2 show that the Flugge and the Love theory produce very similar results. Furthermore, both of these theories are in great agreement with the experimental results especially in the case of the axisymmetric and beam-like modes (compared to other theories) which are of great importance acoustically, and even from vibration point of view. Looking at Table 3 however, it is clear that these two theories endure their highest errors at *n*=2 modes.

The wave propagation approach yields inaccurate frequencies for all beam-like modes, however for *n*=2, 3 and 4 modes, it gives results with adequate accuracy with exceptions in modes; (*m,n*)={{(6,3),(4,2)}}. Whereas, the wave propagation seems to be a good solution for the axisymmetric modes.

Yu’s simplification of the Flugge theory behaves much like the original Flugge theory itself. Though Yu’s simplification of the Flugge has an addition benefit of a much straightforward characteristic equation compared to the original theory but, it is definitely not valid for axisymmetric modes, producing complex frequency numbers for these modes. This is due to the fact that in Eq. (24) by considering *n*=0 the wavelength ratio k_a^2/n^2 goes to infinity, which is definitely vice versa of Yu’s assumption. Therefore as it can be seen Yu’s simplification is not applicable for axisymmetric modes. In Table 3 it is also observed that Yu’s simplification yields similar errors with the original Flugge theory itself for nearly all modes except at (*m,n*)={{(2,1)}}, in which compared to the Flugge theory a high rise in the error is seen. Such behavior is because at this mode the wavelength ratio is $k_a^2/n^2 = 0.08$ which does not satisfy Yu’s assumption (Eq. (24)) greatly, compared to other modes which normally yield wavelength ratios less than 0.01. Therefore, when dealing with Yu’s assumption one must consider wavelength ratios (k_a^2/n^2) of each mode to see whether the assumption is valid or not.

Finally, the simplified Flugge theory based on the neglect of tangential inertia was considered. This simplification causes an increase in all the frequencies (associated with radial motion). It can be observed from Table 4, that the first axisymmetric mode; (*m,n*)={{(1,0)}} has a modal amplitude *A/C*=3.58, which contributes primarily to a longitudinal vibration. However, based on this theory by neglecting tangential inertia, a mode associated with primarily radial motion has been considered, which is 104 97 Hz, as reported in Table 2. This frequency is called the ring frequency of a cylindrical shell which plays an important role in the acoustic engineering. Therefore, this theory predicts a radial frequency for the axisymmetric mode, although the dominant motion in this mode is a longitudinal motion. The simplification causes the beam-like mode frequencies to increase highly, compared to all other shell-like modes (*n* > 1). This is because the neglect of tangential inertia in the beam-like modes causes half of the shell’s inertia to be left out of calculations; therefore, the shell is replaced by another shell which has half of its initial mass. Thus, as the frequency depends upon the square root of the mass, a frequency $\sqrt{2}$ times greater is obtained. Moreover, for the beam-like (*n*=1) modes as shown in Table 4 we

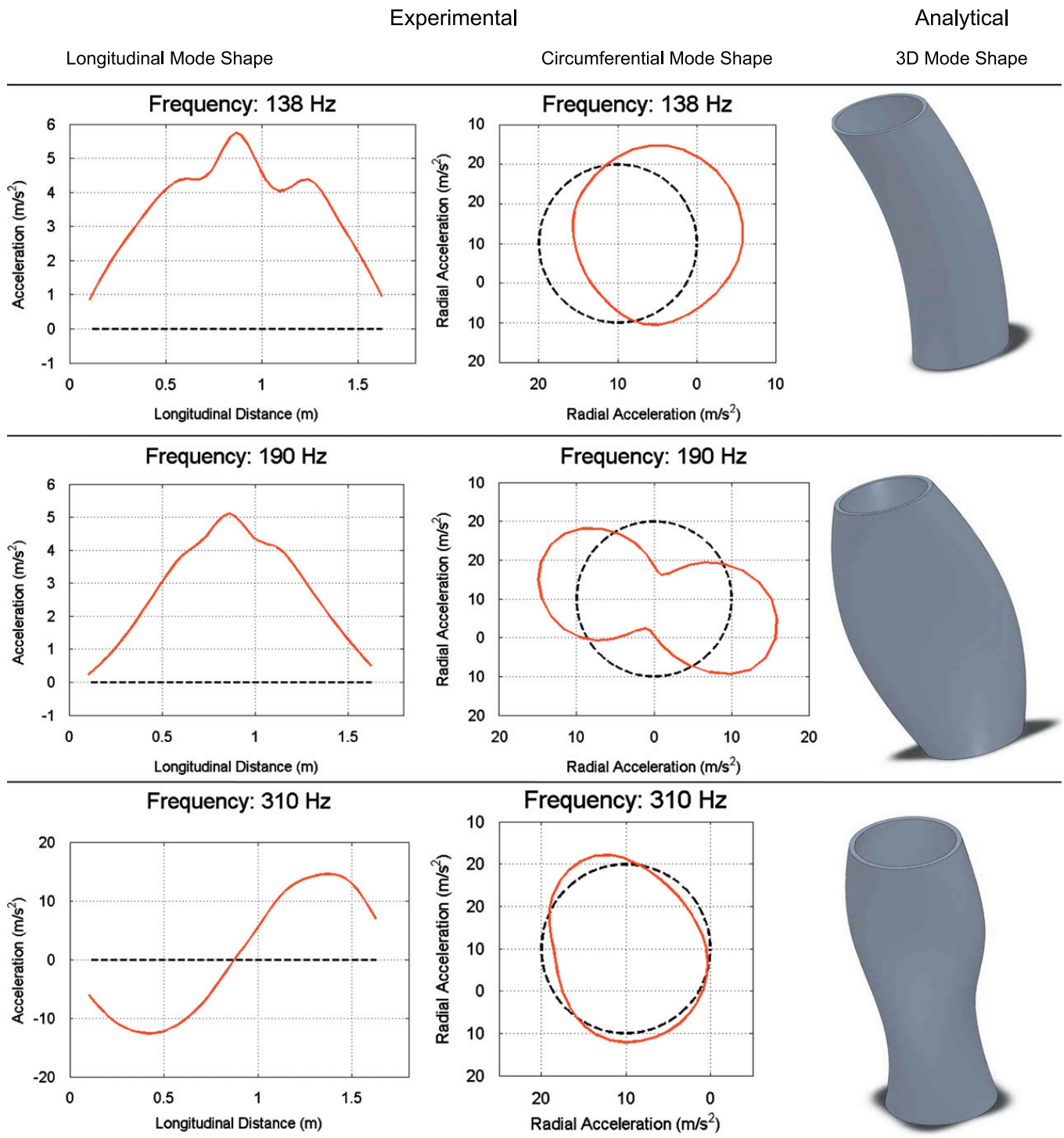


Fig. 8. Mode shape comparisons: longitudinal mode shapes, circumferential mode shape, 3D mode shape. Dashed lines (---) represent the unchanged shape of the tube and the solid lines (—) represent the mode shape. (It is to note that all accelerations are based on a reference point.)

have; $B/C \approx 1$. As a result in these modes the torsional motion is the same as the radial motion, causing some tangential displacements, though not as high as in the axisymmetric mode.

According to Table 4, it can be concluded that the radial motions get weaker at; $(m,n) = \{(1,0), (1,1), (2,1), (4,2)\}$ modes, where the shells motion gets closer to a more axial or torsional vibration by having modal amplitude ratios of $A/C > 0.1$ and $B/C > 0.5$. As a result, at these modes some inplane (tangential) displacements take place. It would be interesting to point out; that at these frequencies the wave propagation and the neglect of tangential inertia methods result in high errors. Therefore these two theories are not valid for modes in which inplane (tangential) displacements take place.

It is remarkable that the fundamental frequency was predicted around 138 Hz by the Flugge and the Love theory and almost 142 Hz by Yu's simplification, which is in good agreement with the experimental result, in $(m,n) = \{(1,1)\}$ mode.

Table 4
Modal amplitude ratios according to Eqs. (18) and (19).

Longitudinal wave parameter	Circumferential wave parameter	Frequency (Hz)	Longitudinal ratio	Circumferential ratio
m	n	Experiment	$ A/C $	$ B/C $
1	0	842.50	3.58	0
1	1	138.40	0.13	1.01
2	1	464.70	0.24	1.02
1	2	190.30	0.03	0.50
2	2	310.50	0.07	0.50
3	2	496.60	0.09	0.51
4	2	679.80	0.12	0.51
1	3	502.20	0.02	0.33
2	3	477.00	0.03	0.33
3	3	558.90	0.04	0.34
4	3	638.30	0.06	0.34
5	3	782.00	0.07	0.34
6	3	833.80	0.08	0.34
1	4	884.40	0.01	0.25
2	4	887.00	0.02	0.25
3	4	981.60	0.03	0.25
4	4	945.80	0.03	0.25
5	4	964.70	0.04	0.25

However, the other two theories, show a higher frequency at a different mode; $(m,n)=\{(1,2)\}$. Therefore, it can be concluded that the wave propagation approach and the simplified Flugge theory based on the neglect of tangential inertia are not accurate approaches for low frequency analysis of long thin-walled shells ($L/R=22.67$, $R/h=51.72$). In Table 4 one can notice that the axisymmetric mode is completely axial and the beam-like modes are primarily radial and torsional, however, for higher modes and as the circumferential wave parameter n increases the motions become largely radial. The same could be said for Table 3, in which as n increases the theories especially the Love and Flugge endure less error. Hence, all theories predict natural frequencies more accurately for modes of higher circumferential wave parameter n , in which the radial motion is more dominant.

As it can be seen from Eq. (5) the axial wavenumber is dependent upon the circumferential wavenumber n , meaning the circumferential and the axial motions to be coupled with each other. However, when using beam functions to determine the axial wavenumber, k_m is assumed to be a known variable independent from the circumferential wave parameter n . This assumption will certainly generate some errors by itself. Apart from theoretical errors, some errors occur because of the shell's imperfections, causing experimental errors which are not related to theories at all.

A very interesting observation was noticed experimentally in the axisymmetric mode; $(m,n)=\{(1,0)\}$ and the three modes surrounding it; $(m,n)=\{(6,3),(1,4),(2,4)\}$. For all these modes the final mode shape is a combination of two or more modes; one is the corresponding mode itself and the others are the three other modes mentioned above. This phenomenon was studied theoretically by Bozich [16], in which he found for the axisymmetric and the beam-like modes that as L/mR is increased (long shells), the motions become more axial and mixed. Such a phenomena was experienced experimentally in our shell, especially for axisymmetric mode; $(m,n)=\{(1,0)\}$, as shown in Fig. 9. It is clear in this figure that the shell does not produce a proper $n=0$ circumferential shape similar to that shown in Fig. 2. This is because the axisymmetric mode has an amplitude ratio of $A/C=3.58$, corresponding to a primarily axial vibration as shown in Table 4. Therefore as the tube is excited by an axial vibration the lower half of the circle tends to move upwards in phase with the upper half motion. Though, the radial and torsional motions of the lower half deflect this section downwards, but since the axial motion is dominant, it actually neutralizes these downward deflections. Consequently it is observed in Fig. 9, that for this axisymmetric mode the upper half of the circle produces a proper $n=0$ mode shape, due to the fact that in the upper half all three motions are in phase, in contrary to the lower half where the axial motion is out of phase with the radial and torsional motions. Hence combinations of all these motions produce a complex general mode shape for the axisymmetric mode.

For better understanding of the modal amplitude ratio (A/C and B/C) behaviors of the shell, Fig. 10 has been plotted, for low frequency modes of $m=1$. In this figure at only $(m,n)=\{(1,0)\}$ mode, A/C is bigger than one and yields a positive number. In this mode some abnormal behaviors were observed from the shell. For modes of $n > 2$ it can also be seen that the motion tends to become completely radial.

An $n-\Omega$ diagram for different values of m has been plotted for the shell under investigation ($L/R=22.67$, $R/h=51.72$). The diagram shown in Fig. 11 is according to the Flugge theory. It can be observed from this figure that as m and n increase, the low frequency modes are pushed into narrow frequency bands, increasing the modal density and making mode shape identification harder. According to this figure for modes of $n \geq 5$, all primarily radial natural frequencies nearly lie in the same narrow frequency bands.

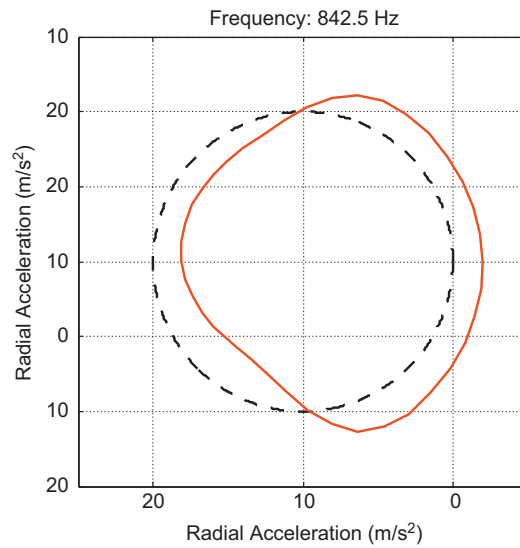


Fig. 9. Experimental circumferential mode shape: first axisymmetric mode $n=0, m=1$ (845 Hz).

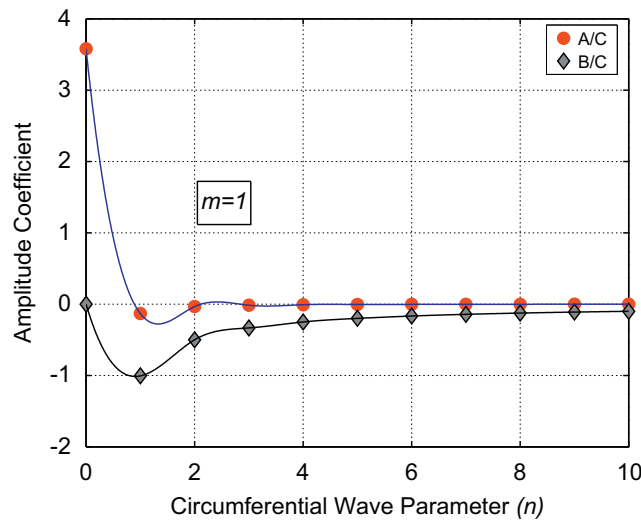


Fig. 10. Modal amplitude ratios for low frequency modes of $m=1$; $L/R=22.67, R/h=51.72, \nu=0.33$.

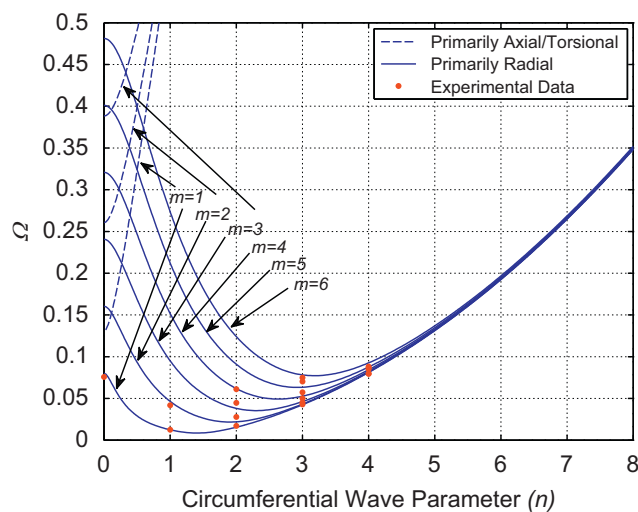


Fig. 11. Variation of non-dimensional frequency parameter Ω with n ; Flugge theory, $L/R=22.67, R/h=51.72, \nu=0.33$.

A more general approach towards shell vibration is made in Fig. 12 by plotting $n-\Omega$ diagram of the Flugge theory for various values of L/mR ($R/h=51.72$). By this figure it is understood for the short shells having ratios of $L/mR \leq 0.2$, that they tend to act more like a ring rather than a beam. This is due to the fact that, for such short shells the tangent of the $n-\Omega$ diagram is positive, for all values of n . Moreover, this figure also serves to emphasize that for a circular cylindrical shell of given length and radius, the lowest (fundamental) frequency ($m=1$), occurs for $n \geq 2$, unless $L/R \geq 20$. Therefore for long shells ($L/R \geq 20$) the minimum frequency occurs for beam-like modes ($n=1$), which shows that it would act more like a beam rather than a ring.

A final inspection into shell vibrations is given by comparison of beam-like modes ($n=1$) of a circular cylindrical shell with that of a transverse vibration of a beam with a cylindrical cross section. For a beam whose cross section is a cylindrical shell tube of thickness h and mean radius R , the area A and the inertia moment of cross section I we have:

$$A' = 2\pi R h \quad I = \pi R^3 h (1 + 3\beta) \tag{28}$$

where β is given by Eq. (10). The transverse vibration frequencies of a simply supported beam are then to be found by

$$\omega_{\text{beam}}^2 = \frac{EI}{\rho A} k_m^4 \tag{29}$$

The beam-like modes of a circular cylindrical shell, used in the experimental setup ($L/R=22.67$), are calculated by the Flugge theory, Eq. (9), and also by the beam function equation, Eq. (29). Results are plotted in Fig. 13. The error curve produced by using the beam function is also plotted in Fig. 14. By Fig. 13 it is really interesting to see how for small values of m/L , the beam curve is in pretty good agreement with the shell curve. According to Fig. 14 for small ratios of $m/L \leq 1.2$, nearly an error less than 10% is obtained when one decides to calculate beam-like modes of a shell by means of beam

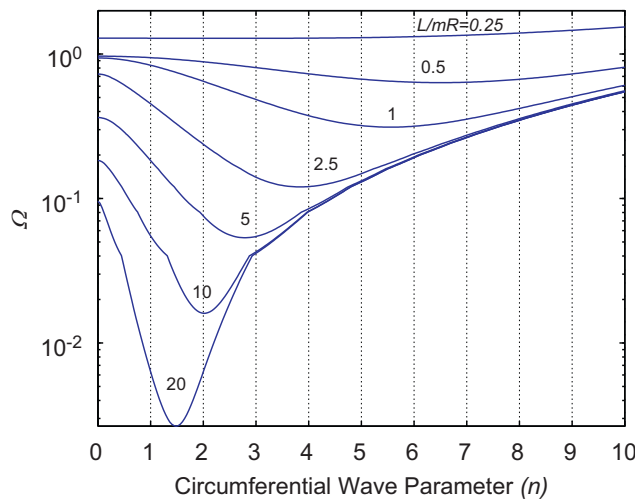


Fig. 12. Variation of non-dimensional frequency parameter Ω with n (with variable L/mR ratios); Flugge theory, $R/h=51.72$, $\nu=0.33$.

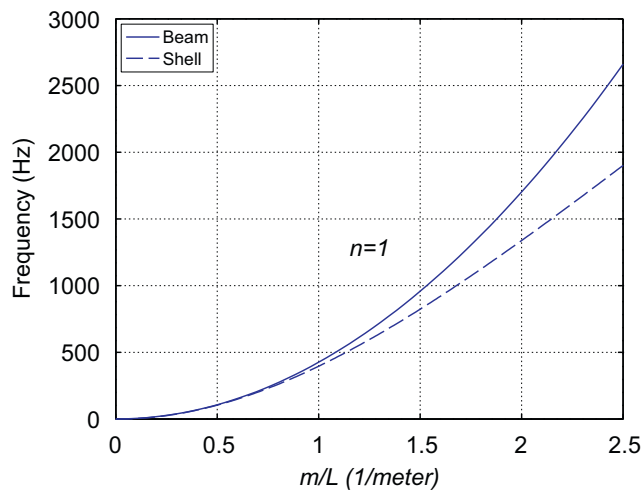


Fig. 13. Beam-like modes of a shell according to beam functions and shell functions; $R/h=51.72$, $\nu=0.33$.

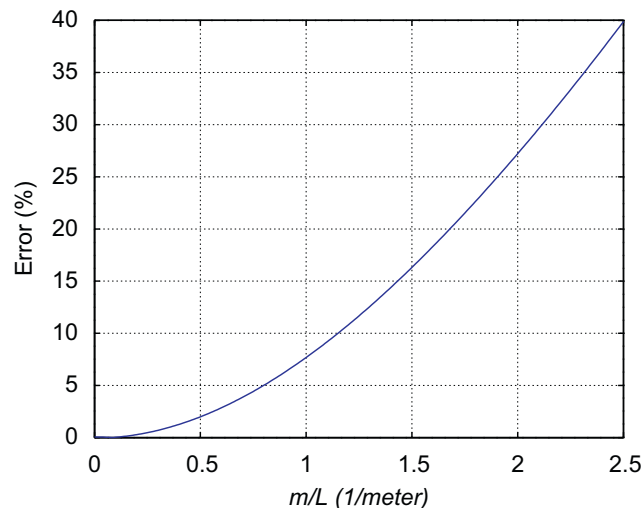


Fig. 14. Error curve for calculating shell beam-like modes of a shell by beam functions; $R/h=51.72$, $\nu=0.33$.

functions instead of the shell functions discussed earlier. Hence, if a beam-like mode of a long shell with such dimensions; $R/h=51.72$, fulfills the postulate; $m/L \leq 1.2$, one can use the beam function instead of the shell function to calculate the natural frequency.

It was observed that from Fig. 12, for long shells having ratios of $L/R \geq 20$ the fundamental frequency would occur at a beam-like ($n=1$) mode. In addition to this, such shells usually satisfy the beam function assumption which was stated earlier; $m/L \leq 1.2$. Therefore for shells of; $R/h=51.72$ and $L/R \geq 20$, it is accurate and much straightforward to use beam functions instead of shell functions to predict the fundamental (lowest) natural frequency. Two of our shell's beam-like modes; $(m,n)=\{(1,1),(1,3)\}$, satisfied the assumption; $m/L \leq 1.2$, their frequencies were therefore calculated by means of a beam function with similar characteristics. Good results were obtained, especially for the shells' fundamental frequency; $(m,n)=\{(1,1)\}$, in which by using the beam theory a frequency of 142.60 Hz yielded, which endures an error less than 2.5%. As mentioned earlier, the wave propagation approach and the simplified Flugge theory based on the neglect of tangential inertia do not predict frequencies of the beam-like modes accurately. Thus the errors of these two theories mostly caused at beam-like modes, can be corrected easily by using the beam function instead.

11. Conclusion

In this work both theoretical and experimental analyses were carried out on a long circular cylindrical shell. A total of 18 modes, consisting of all the three main mode groups (axisymmetric, beam-like and asymmetric) were found under a frequency range of 0–1000 Hz, by only applying acoustical excitation. Acoustical excitation results were compared with those obtained from contact excitation. It was discovered that if one uses contact methods, several exciting points are required to obtain all modes; whereas with acoustical excitation only one acoustical source location for the excitation is needed. Furthermore, acoustical excitation produced much better results, compared with contact excitation, in the frequency band 0–3200 Hz.

A study was then conducted to compare predictions made by five analytical methods and experimental results for the case of a long circular cylindrical shell. By studying the direct solutions obtained from the Flugge and Love theories, accurate results were obtained, especially for axisymmetric and beam-like modes. Yu's simplification applied to the Flugge theory also appears to provide an accurate approach, with no substantial errors induced, except for axisymmetric modes, where Yu's assumption is not valid. Two other methods; (1) the wave propagation and (2) the neglect of tangential inertia, however, were found to be inadequate for primarily longitudinal and torsional modes. Longitudinal and torsional dominant modes do not occur at low frequencies for short or medium length cylindrical shells. However, for a long shell similar to that used in our experiment, such modes were observed at low frequencies, both theoretically and experimentally. These longitudinal and torsional motions usually occur in axisymmetric and beam-like modes. A method was therefore used to reduce errors at these modes, by calculating beam-like modes of the shell using simple beam functions. Errors were reduced substantially, by substituting these results into either of the two methods discussed above. Moreover, it was observed experimentally that for non-dominant radial modes of a long cylindrical shell, complex motion occurs in which combination of one or two modes is normally present. This is due to the fact that, for these modes, strong dominant modal motion does not occur. Therefore, for such motion there is no dominant characteristic motion, which leads to a complex mode shape, which cannot be predicted accurately by theory.

Appendix A

A.1. Differential operators L_{ij} according to the Flugge theory

$$\begin{aligned}
 L_{11} &= R^2 \frac{\partial^2}{\partial x^2} + (1 + \beta) \frac{(1 - \nu)}{2} \frac{\partial^2}{\partial \theta^2} - \frac{\rho h R^2}{D} \frac{\partial^2}{\partial t^2}, & L_{13} &= \nu R \frac{\partial}{\partial x} - R^3 \beta \frac{\partial^2}{\partial x^3} + \frac{(1 - \nu)}{2} R \beta \frac{\partial^3}{\partial x \partial \theta^2} \\
 L_{12} &= \frac{1 + \nu}{2} R \frac{\partial^2}{\partial x \partial \theta}, & L_{21} &= L_{12} \\
 L_{22} &= \left[\frac{1 - \nu}{2} R^2 + \frac{3}{2} (1 - \nu) R^2 \beta \right] \frac{\partial^2}{\partial x^2} + \frac{\partial^2}{\partial \theta^2} - \frac{\rho h R^2}{D} \frac{\partial^2}{\partial t^2}, & L_{23} &= -\frac{(3 - \nu)}{2} R^2 \beta \frac{\partial^3}{\partial x^2 \partial \theta} + \frac{\partial}{\partial \theta}, \\
 L_{31} &= L_{13}, & L_{32} &= L_{23} \\
 L_{33} &= 1 + (1 + \nabla^4 + 2 \frac{\partial^2}{\partial \theta^2}) \beta + \frac{(1 - \nu^2) \rho R^2}{E} \frac{\partial^2}{\partial t^2}, \\
 D &= \frac{Eh}{1 - \nu^2}, & \beta &= \frac{h^2}{12R^2}.
 \end{aligned}$$

A.2. Differential operators L_{ij} according to the Love theory

$$\begin{aligned}
 L_{11} &= R^2 \frac{\partial^2}{\partial x^2} + \frac{1 - \nu}{2} \frac{\partial^2}{\partial \theta^2} - \frac{\rho h R^2}{D} \frac{\partial^2}{\partial t^2}, & L_{12} &= \frac{1 + \nu}{2} R \frac{\partial^2}{\partial x \partial \theta}, \\
 L_{13} &= \nu R \frac{\partial}{\partial x}, & L_{21} &= L_{12}, \\
 L_{22} &= \left[\frac{1 - \nu}{2} R^2 + (1 - \nu) R^2 \beta \right] \frac{\partial^2}{\partial x^2} + 2 \frac{\partial^2}{\partial \theta^2} - \frac{\rho h R^2}{D} \frac{\partial^2}{\partial t^2}, & L_{23} &= \left[-\frac{\partial^3}{\partial x^2 \partial \theta} - \frac{\partial^3}{\partial \theta^3} \right] \beta + \frac{\partial}{\partial \theta}, \\
 L_{31} &= L_{13}, & L_{32} &= \left[-(2 - \nu) R^2 \frac{\partial^3}{\partial x^2 \partial \theta} - \frac{\partial^3}{\partial \theta^3} \right] \beta + \frac{\partial}{\partial \theta}, \\
 L_{33} &= 1 + (\nabla^4) \beta + \frac{(1 - \nu^2) \rho R^2}{E} \frac{\partial^2}{\partial t^2}, \\
 D &= \frac{Eh}{1 - \nu^2}, & \beta &= \frac{h^2}{12R^2}.
 \end{aligned}$$

A.3. Coefficients of the Flugge characteristic equation (Eqs. (9) and (22))

$$\begin{aligned}
 p_4 &= 1 + \frac{1}{2} (3 - \nu) (n^2 + k_m^2) + \beta (n^2 + k_m^2)^2, & p_2 &= \frac{1}{2} (1 - \nu) \left[(3 + 2\nu) k_m^2 n^2 + n^2 + (n^2 + k_m^2)^2 + \frac{(3 - \nu)}{(1 - \nu)} \beta (n^2 + k_m^2)^3 \right], \\
 p_0 &= \frac{1}{2} (1 - \nu) \left[(1 - \nu^2) k_m^4 + \beta (n^2 + k_m^2)^4 \right] + \frac{\beta}{2} (1 - \nu) \left[\frac{2(2 - \nu) k_m^2 n^2 + n^4 - 2\nu k_m^6 - 6k_m^4 n^2}{-(4 - \nu) k_m^2 n^4 - 2n^6} \right], \\
 \bar{p}_2 &= \frac{(1 - \nu)}{2} (n^2 + k_m^2)^2.
 \end{aligned}$$

A.4. Coefficients of the Love characteristic equation (Eq. (12))

$$\begin{aligned}
 a_4 &= -\left[\frac{E}{\rho(1 - \nu^2)R^2\omega} \right]^2 \frac{1}{\rho h} [M_{11} + M_{22} + M_{33}], \\
 a_2 &= -\left[\frac{E}{\rho(1 - \nu^2)R^2\omega} \right] \frac{1}{(\rho h)^2} [M_{11}M_{22} + M_{33}M_{22} + M_{33}M_{11} - M_{23}^2 - M_{12}^2 - M_{13}^2], \\
 a_0 &= -\frac{1}{(\rho h)^3} [M_{11}M_{23}^2 + M_{13}^2M_{22} + M_{33}M_{12}^2 + 2M_{12}M_{23}M_{13} - M_{11}M_{22}M_{33}], \\
 M_{11} &= \left(\frac{Eh}{1 - \nu^2} \right) \left(k_m^2 + \frac{(1 - \nu)n^2}{2R^2} \right), & M_{22} &= \left(\frac{Eh}{1 - \nu^2} + \frac{D'}{R^2} \right) \left(\frac{(1 - \nu)}{2} k_m^2 + \frac{n^2}{R^2} \right), \\
 M_{33} &= D' \left(k_m^2 + \frac{n^2}{R^2} \right)^2 + \frac{1}{R^2} \left(\frac{Eh}{1 - \nu^2} \right), & M_{12} &= M_{21} = \left(\frac{Eh}{1 - \nu^2} \right) \frac{1 + \nu}{2R} k_m n, \\
 M_{13} &= M_{31} = \left(\frac{Eh}{1 - \nu^2} \right) \frac{\nu}{R} k_m, & M_{23} &= M_{32} = \left(\frac{Eh}{1 - \nu^2} \right) \frac{n}{R^2} - \frac{D'n}{R^2} \left(k_m^2 + \left(\frac{n}{R} \right)^2 \right), & D' &= \frac{Eh^3}{12(1 - \nu^2)}.
 \end{aligned}$$

References

- [1] W. Leissa, *Vibration of Shells (NASA SP-288)*, US Government Printing Office, Washington, DC, 1973.
- [2] M. Amabili, M.P. Paidoussis, Review of studies on geometrically nonlinear vibrations and dynamics of circular cylindrical shells and panels, with and without fluid structure interaction, *Applied Mechanics Reviews* 56 (2003) 349–381.
- [3] A.E.H. Love, On the small free vibrations and deformations of thin shells, *Philosophical Transactions of the Royal Society London* 179A (1888) 491–546.
- [4] W. Flugge, *Stresses in Shells*, Springer, New York, 1973.
- [5] W. Soedel, *Vibrations of Shells and Plates*, 3rd ed., Marcel Dekker, Inc., 2004.
- [6] K. Forsberg, *A Review of Analytical Methods used to Determine the Modal Characteristics of Cylindrical Shells (NASA CR-613)*, National Aeronautics and Space Administration, Washington, DC, 1966.
- [7] A. Harari, Wave propagation in a cylindrical shell with joint discontinuity, *Shock and Vibration Bulletin* 48 (1978) 193–198.
- [8] C.R. Fuller, The effect of wall discontinuities on the propagation of flexural waves in cylindrical shells, *Journal of Sound and Vibration* 75 (1981) 53–61.
- [9] X.M. Zhang, G.R. Liu, K.Y. Lam, Vibration analysis of thin cylindrical shells using wave propagation approach, *Journal of Sound and Vibration* 239 (2001) 397–403.
- [10] X.B. Li, Study on free vibration analysis of circular cylindrical shells using wave propagation, *Journal of Sound and Vibration* 311 (2008) 667–682.
- [11] Y.Y. Yu, Free vibrations of thin cylindrical shells having finite lengths with freely supported and clamped edges, *Journal of Applied Mechanics* 22 (1955) 547–552.
- [12] V.I. Weingarten, Free vibration of thin cylindrical shells, *Journal of the American Institute of Aeronautics and Astronautics* 2 (1964) 717–722.
- [13] R.N. Arnold, G.B. Warburton, The flexural vibrations of thin cylinders, *Proceedings of the Institution of Mechanical Engineers* 167 (1953) 62–80.
- [14] F. Pellicano, Vibrations of circular cylindrical shells: theory and experiments, *Journal of Sound and Vibration* 303 (2007) 154–170.
- [15] M. Amabili, *Nonlinear Vibrations and Stability of Shells and Plates*, Cambridge University Press, 2008.
- [16] W.F. Bozich, The vibration and buckling characteristics of cylindrical shells under axial load and internal pressure, AFFDL-TR-67-28, 1967.